

See discussions, stats, and author profiles for this publication at: <https://www.researchgate.net/publication/231646776>

Understanding Acetaldehyde Thermal Chemistry on the TiO₂ (110) Rutile Surface: From Adsorption to Reactivity

ARTICLE *in* THE JOURNAL OF PHYSICAL CHEMISTRY C · JANUARY 2011

Impact Factor: 4.77 · DOI: 10.1021/jp110696f

CITATIONS

8

READS

32

4 AUTHORS, INCLUDING:



[Jose j. Plata](#)

Duke University

22 PUBLICATIONS 231 CITATIONS

SEE PROFILE



[Antonio M Márquez](#)

Universidad de Sevilla

84 PUBLICATIONS 1,343 CITATIONS

SEE PROFILE



[Javier Fdez Sanz](#)

Universidad de Sevilla

62 PUBLICATIONS 1,614 CITATIONS

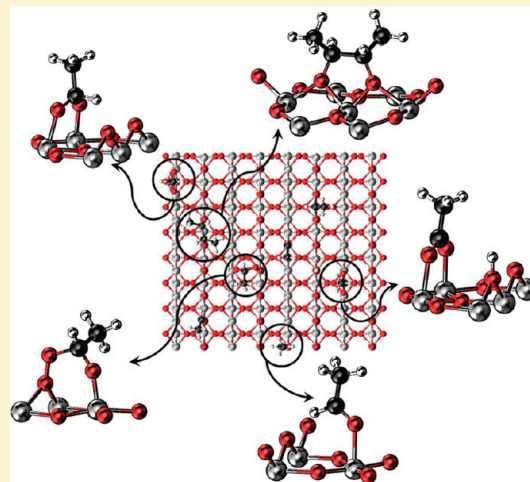
SEE PROFILE

Understanding Acetaldehyde Thermal Chemistry on the TiO_2 (110) Rutile Surface: From Adsorption to Reactivity

José Javier Plata, Veronica Collico, Antonio M. Márquez,* and Javier Fdez. Sanz

Departamento de Química Física, Universidad de Sevilla, Facultad de Química, 41012 Sevilla, Spain

ABSTRACT: Plane-wave pseudopotential density functional theory calculations are used to investigate the details of acetaldehyde adsorption and thermal chemistry on the TiO_2 (110) rutile surface. The adsorption properties of a single acetaldehyde molecule on models of stoichiometric, reduced, and oxidized TiO_2 surfaces are first examined. The experimentally observed shift of the temperature-programmed desorption (TPD) maximum on increasing coverage is rationalized on the basis of the adsorbate to surface bonding mechanism. Examination of the thermal chemistry of acetaldehyde on models of the TiO_2 (110) surface allows one to understand the diffusion of acetaldehyde molecules on the surface and the formation of butene, as is experimentally observed. This reaction takes place through a noncatalytic process where the bridge oxygen vacancies play a fundamental role. The molecular details of the process allow one to explain the low amount of butene found in the experiment. The study of the thermal chemistry of acetaldehyde on models of the TiO_2 (110) oxidized surface allows one to understand the stabilization of acetaldehyde in this surface, compared to the reduced surface, through the formation of O-acetaldehyde surface complexes. One of these complexes is found to undergo an easy and not reversible transformation to a highly stable surface acetate, allowing one to rationalize the high temperature required to desorb acetate from this surface and the low quantity of acetate found experimentally.



INTRODUCTION

Titanium dioxide (TiO_2) is a material that, due to its versatility and the multitude of its applications in catalysis, photocatalysis, solar cells, waste remediation, and biocompatible materials, has received considerable attention in the literature over the years. In particular, the (110) surface of rutile, the thermodynamically most stable structural TiO_2 polymorph, has become a model system in surface science studies of metal oxide surfaces.^{1–7}

The TiO_2 (110) surface consists of alternating rows along the [001] direction of 2-fold coordinated bridging oxygen atoms (O_b) and channels that expose both 5-fold coordinated Ti atoms (Ti_{5c}) and in-plane 3-fold coordinated oxygen atoms (O_{3c}) also referred to as basal oxygen atoms, see Figure 1. The Ti_{5c} atoms act as Lewis acid sites for the adsorption of molecules and the O_b atoms as Brönsted basic sites, which can coordinate an H atom from adsorbates. By heating under vacuum at temperatures of about 800 K a few percent of the O_b atoms can be removed. The density of the resulting O_b vacancies (V_O) is somehow dependent on specific experimental conditions, but typical experiments quantify their concentration as 7–12%. The reactivity of this reduced surface is largely dominated by these point defects as has been shown by different experimental and theoretical studies.^{1,4,7}

The interaction of O_2 with this reduced surface produces a substrate with an excess of oxygen that shows a complex chemistry, involving both atomic and molecular forms of oxygen at the

surface.^{6,8,9} For example, O_2 has been shown to adsorb molecularly at V_O sites below 150 K but dissociates at higher temperatures, leaving an O atom healing the vacancy and an O_{ad} adatom on the Ti channel.^{10,11} Recent STM studies have revealed a second mechanism for O_2 dissociation at the Ti_{5c} channels, leading to formation of pairs of O_{ad} adatoms at temperatures close to ambient.¹² The authors of this study have linked this mechanism of O_2 dissociation to the presence of Ti interstitials near the surface. In either case, the reactivity of the TiO_2 (110) surface has been found to be greatly modified by the presence of the O_{ad} adatoms generated by O_2 dissociation.^{10,11,13,14}

The heterogeneous chemistry of surface-adsorbed organic compounds is a topic of considerable interest in heterogeneous catalysis, nanoscience, solar energy conversion, environmental science, and public health. In particular, the surface chemistry and photochemistry of acetaldehyde has been the subject of diverse studies motivated by both applied and fundamental reasons. Acetaldehyde may be used for the catalytic production of acetone, diethyl ketone, ethanol, crotonaldehyde, butene, and butadiene.^{15,16} It is also commonly found as an usual atmospheric pollutant, with potential carcinogenic effects, as a consequence of its use as an additive or a byproduct of use of ethanol as an

Received: November 9, 2010

Published: January 27, 2011

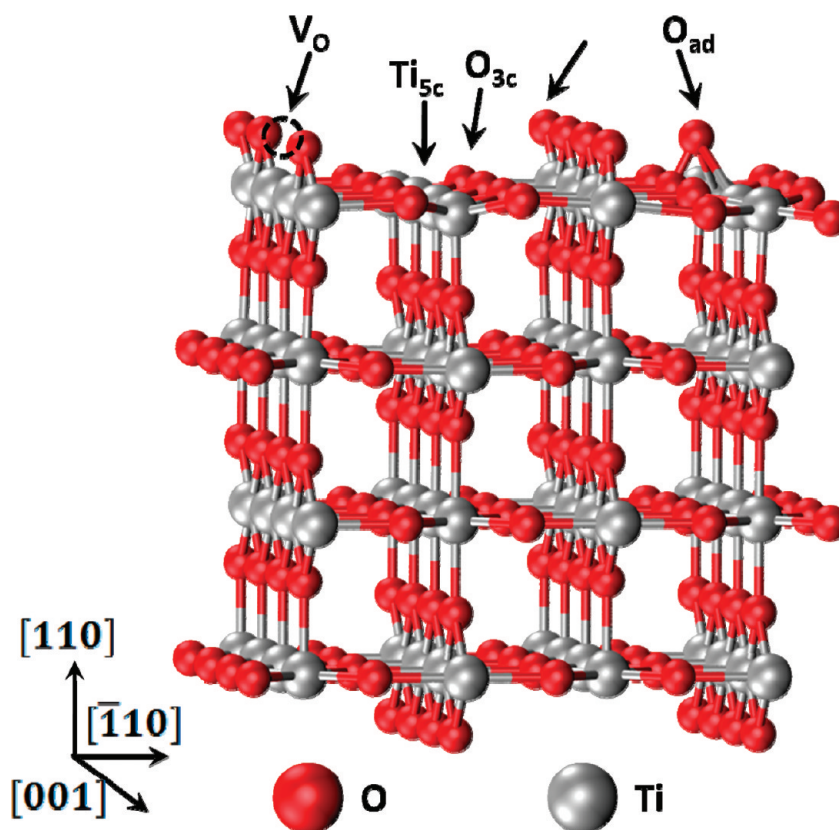


Figure 1. 4×2 supercell model of a TiO_2 (110) rutile surface with four O–Ti–O layers; the two top layers are optimized, and the two lower layers are kept frozen.

automotive fuel.^{17,18} The surface chemistry and photochemistry of acetaldehyde on diverse TiO_2 surfaces is a topic of recurrent interest in the literature (see refs 19–22 and references therein). In one of these studies²¹ Zehr and Henderson investigated the photochemistry of acetaldehyde on the TiO_2 (110) surface. They examined the interaction of acetaldehyde with reduced and oxidized TiO_2 (110) surfaces using thermal programmed desorption (TPD) in an ultra-high-vacuum (UHV) chamber and obtained details of the thermal chemistry of acetaldehyde at these surfaces. TPD data indicate a coverage dependence in the binding energy of acetaldehyde, even at low coverage (<0.5 ML), that is tentatively ascribed to the presence of adsorbate–adsorbate steric repulsions. At the reduced (UHV annealed) surface no specific adsorption state associated to bridge oxygen vacancies is detected. Reductive coupling of acetaldehyde to butene is observed but only in a proportion of 1–2% of the applied acetaldehyde dosing (1.4 ML). No other reaction products are observed at the reduced surface. On oxidized TiO_2 (110) surfaces a significant stabilization of the TPD traces of acetaldehyde is observed at low coverage that is assigned to formation of some acetaldehyde–surface oxygen complex. Acetate formation is observed as a minor reaction channel on this surface, but it is argued that the barrier for acetate formation is quite low, because O_2 dosed at room temperature seems to have enough internal energy to initiate formation of acetate. However, the vast majority of adsorbed acetaldehyde is observed to desorb molecularly from this surface in TPD.

We focus this study on understanding and rationalizing, at a molecular level, the surface adsorption energetic and reactivity of acetaldehyde at the TiO_2 (110) rutile surface at low coverage.

After briefly presenting the necessary computational details about the models and methodology used, we will start by examining the adsorption energetics and geometries at the lower coverage studied on models of the ideal (stoichiometric), reduced, and oxidized TiO_2 (110) surfaces, including the effects of an approximate treatment of the electron localization on the Ti 3d states through a DFT+U approach. Later, the coverage effects on the acetaldehyde to surface binding energies will be examined. In a final section the thermal chemistry of acetaldehyde on the TiO_2 (110) surface will be explored: experimental facts like formation of butene on the reduced surface or traces of acetate found on TPD of acetaldehyde on the oxidized TiO_2 (110) surface will be rationalized. In the final section we will establish the conclusions of our work.

■ SURFACE AND COMPUTATIONAL MODEL

All calculations were performed using a slab model for the rutile TiO_2 (110) surface with the VASP 4.6 code.^{23–25} The energy is obtained in these calculations using the projector augmented wave (PAW) method^{26,27} and the generalized gradient approximation (GGA) implementation of DFT as proposed by Perdew et al.²⁸ The electronic states were expanded using a plane-wave basis set with a cutoff of 400 eV. The forces on the ions were calculated through the Hellmann–Feynman theorem as the partial derivatives of the free energy with respect to the atomic coordinates, including the Harris–Foulkes correction to the forces.²⁹ This way of calculating the force allows a geometry optimization using the conjugated gradient scheme. Iterative relaxation of the atomic positions was stopped when the forces on the atoms were less than 0.05 eV/Å. Desorption and reaction

energetic barriers have been located using the climbing image version of the nudged elastic band algorithm.³⁰

The TiO₂ (110) surface was treated by a slab model with three-dimensional boundary conditions, as shown in Figure 1. We used a (4 × 2) supercell where adsorption of a single acetaldehyde molecule represents a coverage of $\theta = 0.125$ ML (monolayers). The cell was 12 atomic layers thick or four TiO₂ trilayers, as it is known that thicker supercell models gave comparable results in a similar study.³¹ In all cases, the two lower TiO₂ trilayers were kept frozen while the rest of the atoms were allowed to fully relax their atomic positions. The supercell model is separated from their images by a vacuum of 15 Å, considered enough to avoid interaction between the slabs. The optimized lattice parameters for the bulk used were $a = 4.1616$ Å, $c = 2.974$ Å, and $u = 0.304$ Å, with the a and c parameters fixed during the surface atomic positions relaxation. All calculations were performed at the Γ point of the Brillouin zone.

To model the reduced TiO₂ (110) surface, one bridging oxygen atom was removed from the surface, thus representing a 12.5% vacancy concentration, similar to typical experimental conditions. Taking into consideration experimental evidence and previous theoretical calculations,^{8,31–33,10,11} we modeled the oxidized TiO₂ (110) surface by adding one oxygen atom to the Ti_{5c} channel.

Different papers in the recent literature have stressed the importance of an adequate description of the degree of electron localization on TiO₂.^{34–38} Gradient-corrected density functional theory assigns a delocalized character to the excess electrons induced on the TiO₂ surface by defects like O vacancies or the presence of adsorbates due to inherent defects in the functional, like electron self-interaction.^{32,39} An approximate way to enhance electron localization at a reasonable computational cost is the DFT+U model,⁴⁰ which mitigates the problems associated to the self-interaction errors of DFT. However, while DFT+U has been very successful in the description of localized defect states, it has received less attention in reactivity and adsorption studies.^{8,32,41} Thus, we checked the effect of a DFT+U description of Ti 3d states by employing a U value of 4.5 eV, consistent with previous work,⁴² in selected states of the acetaldehyde molecule adsorbed on the TiO₂ (110) surface.

Desorption energies were always computed with respect to an isolated acetaldehyde molecule on a 20 × 20 × 20 Å box as $\Delta E_{\text{bond}} = E_{\text{acetaldehyde/surf}} - (E_{\text{surf}} + E_{\text{acetaldehyde}})$. Thus, negative desorption energies represent bound states, stable with respect to desorption.

RESULTS AND DISCUSSION

Molecular Adsorption and Coverage Effects. Molecular adsorption of acetaldehyde on the TiO₂ (110) surface takes place mainly by interaction of the carbonyl group dipole moment with the surface electric field generated by the Ti cations. The Brønsted acid character of the α -H atom of the acetaldehyde molecule allows for further stabilization by interaction with the surface anions. Molecular adsorption of acetaldehyde has been initially investigated at a coverage of $\theta = 0.125$ ML. Multiple adsorption configurations including atop and bridge sites over the pentacoordinated Ti channel atoms as well as the V_O sites at the reduced surface have been examined. Table 1 summarizes the energetic of acetaldehyde molecular adsorption on stoichiometric, reduced, and oxidized models of the TiO₂ (110) surface at this coverage. The GGA-computed energies show that on the

Table 1. Computed Adsorption Energies (in eV) for a Single Acetaldehyde Molecule (corresponding to a coverage of $\theta = 0.125$ ML) on the Ti Sites of the (110) Rutile Surface

stoichiometric			reduced			oxidized		
site	GGA	GGA+U	site	GGA	GGA+U	site	GGA	GGA+U
Ti _{5c} ^a	−0.83	−1.02	V _O ^b	−1.02	−1.37	Ti _{5c} (c0) ^d	−0.81	−1.00
Ti _{5c} ^b	−0.66	−0.81	V _O ^a	−0.69	−0.86	Ti _{5c} (c1) ^d	−0.79	−1.01
			Ti _{5c} (0) ^c	−0.84	−1.04	Ti _{5c} (0) ^c	−0.68	−0.74
			Ti _{5c} (1) ^c	−0.82	−1.01	Ti _{5c} (1) ^c	−0.78	−1.01

^a The acetaldehyde molecular symmetry plane is perpendicular to the Ob row. ^b The acetaldehyde molecular symmetry plane is parallel to the Ob row. ^c Sites (0) and (1) are, respectively, the first and second neighbors to the V_O site (on the reduced surface) or the O_{ad} adatom (on the oxidized surface). ^d Sites (c0) and (c1) are nonequivalent Ti_{5c} sites on the channel not bearing the O_{ad} adatom on the oxidized surface.

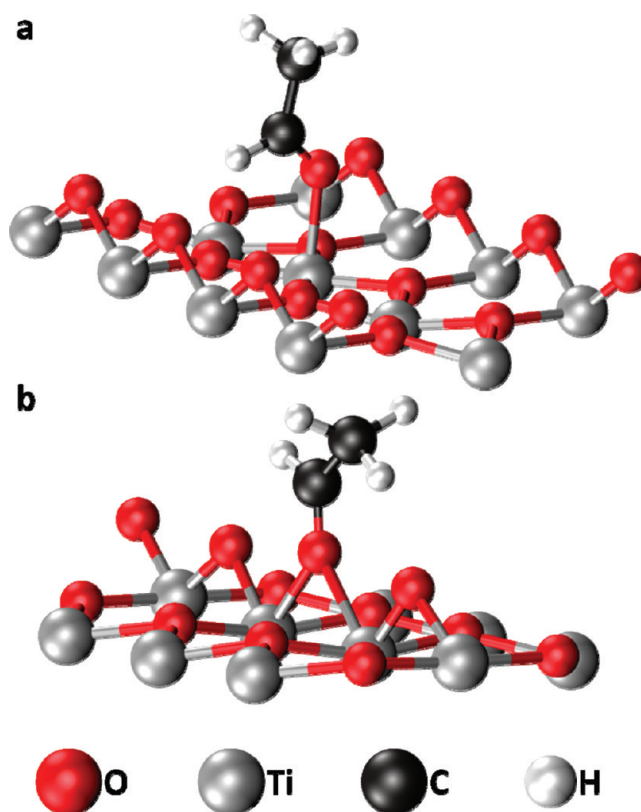


Figure 2. (a) Geometry of acetaldehyde adsorbed on top of the Ti_{5c} site on the stoichiometric surface. (b) Acetaldehyde adsorption geometry at the V_O site on the reduced surface.

stoichiometric surface the most stable molecular adsorption configuration is atop a Ti_{5c} channel site, as shown in Figure 2a. The adsorption energy for this configuration is −0.83 eV, and the distance between the Ti_{5c} atom and the oxygen atom of the carbonyl group is 2.17 Å. The carbonyl C–O bond is elongated with respect to the free acetaldehyde molecule. In the adsorbed state the C–O distance is 1.24 Å, whereas in the isolated acetaldehyde molecule the computed optimized C–O distance is 1.22 Å. The Ti_{5c} is slightly above the channel surface by 0.16 Å. These two data (elongation of the C–O bond and outward

displacement of the Ti_{5c} cation) are indicative of some adsorbate to surface charge transfer that reduces the interaction between the Ti atom and the surface O atoms of its first coordination shell. The Ti–O–C angle is 129° , with the acetaldehyde molecule tilted toward the O_b row, indicating the existence of some hydrogen-bonding interaction between the acetaldehyde α hydrogen and the O_b atom that contributes to stabilize the adsorbed acetaldehyde molecule. On the reduced TiO_2 (110) surface, as expected, the most stable adsorption site is the V_O (see Figure 2b). The most favorable configuration corresponds to insertion of the carbonyl group into the V_O , with the acetaldehyde molecular symmetry plane parallel to the bridging O row. The α hydrogen atom of the acetaldehyde molecule is tilted toward a nearby O_b atom (the H_α –O–C angle is reduced from 119° in free acetaldehyde to 116°). The adsorption energy of the acetaldehyde molecule on this site is -1.02 eV, slightly higher than on the previously discussed Ti_{5c} sites of the stoichiometric surface. The interaction between the acetaldehyde molecule and the Ti_{5c} sites of the reduced surface is quantitatively similar to what has been found on the regular surface. The binding energies for the two nonequivalent Ti_{5c} sites are -0.82 and -0.84 eV; thus, no significant effect is induced by the presence of the nearby vacant site. Similarly, on the oxidized surface, the presence of the O_{ad} adatom only influences neighboring Ti_{5c} sites. The binding energies of the acetaldehyde molecule lie in the -0.78 to -0.81 eV range (at the GGA level) when the acetaldehyde molecule binds on top of a Ti_{5c} site not directly interacting with the surface O_{ad} adatom. If the acetaldehyde molecule binds to one of the two Ti_{5c} atoms attached to the O_{ad} adatom the acetaldehyde surface interaction decreases due to the repulsion between the electronic clouds of the acetaldehyde molecule and the O_{ad} adatom, resulting in a lower binding energy (-0.68 eV).

The relative energetics of acetaldehyde adsorption at $\theta = 0.125$ ML is basically unchanged when an approximate treatment of the electron localization effects through a GGA+U approximation is performed. The computed GGA+U binding energies on the different Ti_{5c} sites and surfaces, displayed in Table 1, are increased by 0.15 – 0.35 eV, but in any case, the relative ordering among the different adsorption configurations is preserved. The binding energy computed for acetaldehyde adsorption on the Ti_{5c} site bonded to the O_{ad} adatom on the oxidized surface does not follow this trend. The binding energy is almost unchanged from -0.68 (GGA) to -0.74 eV (GGA+U). This is probably due to a cancellation of the increased binding to the Ti_{5c} site by a similar increase of the repulsion between the electronic clouds of the acetaldehyde molecule and the O_{ad} adatom.

Experimental TPD data for acetaldehyde desorbing from a UHV annealed TiO_2 (110) surface²¹ shows two peaks at 390 and 320 K for very low coverage. The 390 K peak has a high-temperature tail and saturates at a coverage of ~ 0.01 ML. This feature is most probably related with adsorption at surface defects (steps and corners), taking into account that it saturates at a very low loading. The band at 320 K is highly asymmetric, showing two components: a high-temperature one that saturates at a coverage of about 0.15 ML and a low-temperature component that shifts downward to 260 K with increasing coverage, saturating at a coverage of 0.33 ML. For higher coverage, a poorly resolved new feature develops at 245 K as a low-temperature shoulder of the 320 K band. This feature saturates at a coverage of 1 ML. This downward shift of the 320 K band has been interpreted as consistent with increasing adsorbate–adsorbate repulsions that destabilize the acetaldehyde–surface bond.²¹

Table 2. Computed Desorption Energies (E_{des}) for a Single Acetaldehyde Molecule Desorbing from On-Top Ti_{5c} Sites as a Function of Total Coverage

θ/ML	GGA E_{des}/eV	GGA+U E_{des}/eV
V_O site	-1.02	-1.37
0.125	-0.83	-1.02
0.250 (same channel)	-0.64 to -0.65	-0.86 to -0.88
0.250 (next channel)	-0.70 to -0.75	-0.91 to -0.96
0.375	-0.53 to -0.62	
0.500	-0.43 to -0.51	

However, the trends found on the computed acetaldehyde desorption energies with increasing surface coverage, summarized in Table 2, allow for a reinterpretation of this effect in terms of the acetaldehyde–surface bonding mechanism. The high-temperature tail of the 320 K band that saturates at a surface loading of ~ 0.15 ML can be assigned to molecular desorption of acetaldehyde from O_V sites. The computed GGA desorption energy, -1.02 eV, is consistent with this assignment. Computed acetaldehyde desorption energies from Ti_{5c} sites follow a trend with increasing acetaldehyde coverage that closely matches what is found on the TPD spectrum. At 0.125 ML coverage the computed binding energy of -0.83 eV (at the GGA level) will correspond to a desorption temperature close to the high-temperature tail of the TPD band. The further increase of acetaldehyde coverage in our periodic supercell model to 0.250 ML implies the presence of two distinct adsorbate molecules that can be placed either on the same or in different Ti channels. In both cases, the computed desorption energy for the leaving molecule decreases, in agreement with the observed shift on the TPD band toward lower temperatures, but the decrease is higher if both molecules reside on the same Ti channel. These data can be interpreted in terms of two effects that concurrently operate over the acetaldehyde–surface bonding mechanism. The first contribution, over the long range, is the dipole–dipole repulsions between coadsorbed acetaldehyde molecules that can be mainly responsible for the observed reduction of the binding energy when the acetaldehyde molecules are far apart (i.e., on different Ti_{5c} channels). The second contribution is a small charge transfer that takes place upon acetaldehyde adsorption. On the basis of a Bader charge analysis for the lower acetaldehyde loading, this charge transfer is estimated to be ~ 0.10 e[−]. This electron density goes to the Ti_{3d} band, reducing the acidity of nearby Ti_{5c} sites, and thus the binding energy of newly incoming acetaldehyde molecules. This effect is mainly electronic as there is, almost, no contribution of acetaldehyde–acetaldehyde lateral repulsions: the binding energies computed at 0.250 ML for the two possible arrangements of two adsorbate molecules on the same channel are identical (-0.64 and -0.65 eV). It may be argued that this interpretation has a fundamental flaw: the gradient-corrected DFT functional tends to overestimate the delocalization of the electron density. However, the GGA+U data presented in Table 2 follow the same trend as the GGA results. The computed desorption energies are increased by 0.22 – 0.27 eV, but the relative values are basically the same. Thus, the excessive electron delocalization that may result from the use of the pure GGA approach has no effect on the interpretation of this effect. A further increase of the acetaldehyde loading in our supercell model to $\theta = 0.375$ ML results in a new decrease of the adsorbate–surface binding energy for the

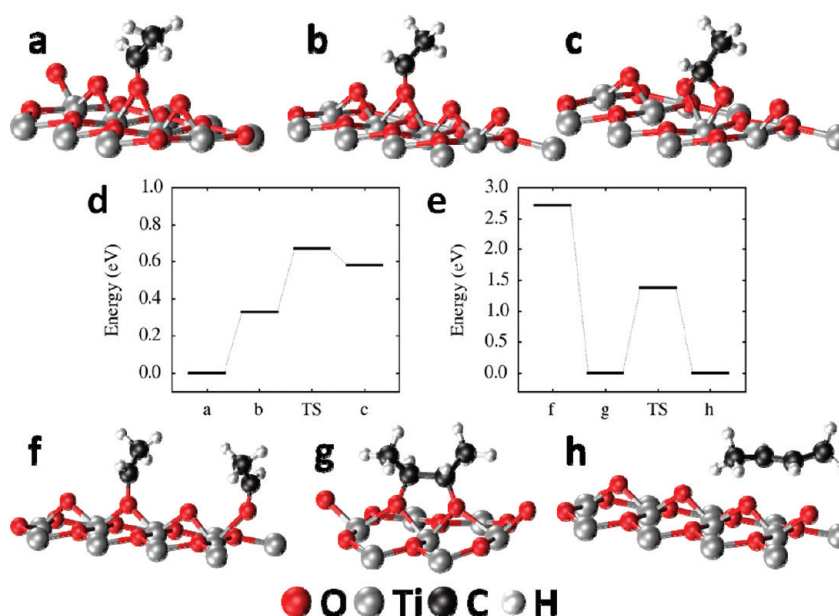


Figure 3. (a) Geometry of acetaldehyde adsorbed at the V_O site on the reduced surface with the molecular symmetry plane parallel to the O_b row. (b) Adsorption geometry at the V_O site with the molecular symmetry plane perpendicular to the O_b row. (c) Acetaldehyde bidentate configuration over the O_b row. (d) Energy profile of the diffusion pathway with the corresponding key states (a–c). (e) Energy profile for the formation and desorption of butene with the corresponding key states (f–h). (f) Initial state for the approach of two acetaldehyde molecules. (g) Geometry of the adsorbed butene complex. (h) Butene molecule desorbing from the surface.

incoming acetaldehyde molecule. In the most stable distribution of acetaldehyde molecules the desorption energy is reduced to -0.62 eV, while in the most crowded one, which corresponds to the leaving acetaldehyde molecules having other two adsorbate molecules on neighboring Ti_{5c} sites, the acetaldehyde–surface binding energy is further reduced to -0.53 eV. This very crowded situation is more likely to happen when the acetaldehyde loading is increased and can be made responsible for the poorly resolved feature that develops, for loading higher than 0.33 ML, as a low-temperature shoulder of the 320 K band on the TPD spectrum.

Thermal Chemistry. On the TiO_2 (110) reduced surface a small fraction (1–2%) of the adsorbed acetaldehyde has been found to decompose resulting in formation of butene.²¹ The TPD trace for butene, formed by the reductive coupling of two acetaldehyde molecules, appears at about 530 K. No other reaction products have been characterized at this surface. No butene formation is detected on the oxidized surface. A detailed understanding of the events leading to formation of butene can be obtained from our density functional theory calculations. In particular, the energy barriers for diffusion, the reductive coupling of the two acetaldehyde molecules, and the desorption of the resulting butene molecule have been studied. The high temperature required to observe butene desorption implies a low acetaldehyde coverage, as most acetaldehyde molecules will desorb from the surface at lower temperatures. Our results show that at low surface coverage V_O is a preferential adsorption site for acetaldehyde on the reduced surface (see Table 1). This preferential adsorption at the V_O sites and the fact that no butene is detected on the oxidized surface suggest that these adsorption sites play a fundamental role on formation of butene. The most stable adsorption configuration does not allow for easy diffusion of acetaldehyde molecules along the O_b row (see Figures 2b and 3a). This is due to the H-bonding interaction between the α -H of the acetaldehyde molecule and a nearby O_b anion. In fact, the

barrier for a concerted diffusion path along the O_b row is found to be 1.6 eV. However, rotation of an alternative configuration with the acetaldehyde molecular symmetry plane perpendicular to the O_b row is easy, as it requires only 0.33 eV (see Figure 3b). The acetaldehyde molecule can now diffuse along the row of bridging oxygen anions by passing through a bidentate configuration (see Figure 3c) that is only less stable than the previous one by 0.25 eV. This step, however, requires surmounting an energetic barrier of 0.34 eV (TS in Figure 3d) as the old C–O bond must be weakened before the new one begins to form. In the next step the acetaldehyde molecule, following back the previously described mechanism, binds to the next O_b atom, leaving behind its carbonyl O atom, healing the original O_V site. Thus, the energy barrier for acetaldehyde diffusion can be estimated to be ~ 0.65 eV. Such an activation barrier can be easily overcome at relatively low temperatures. By diffusion along the row of bridging oxygens two acetaldehyde molecules may collide and, by reductive coupling, form an adsorbed butene molecule (see Figure 3f and 3g). Formation of butene from two adjacent acetaldehyde molecules is found to be an exothermic (-2.72 eV) and barrier-free process (see panel e in Figure 3). Although the computed binding energy of the newly formed butene molecule is 0.6 eV, the desorption process is not barrier free as two C–O bonds have to be broken before the π C–C bond begins to form. The energy barrier required for this process to take place is calculated to be 1.38 eV. On the basis of a simple first-order Redhead analysis⁴³ this desorption energy barrier will closely match the experimentally desorption temperature of 530 K. As indicated at the beginning of this paragraph, the high temperature required for desorption of butene will result in a small amount of acetaldehyde remaining at the surface at these high temperatures. Taking also into account that the density of V_O sites is estimated to be 7–12% and that two V_O sites are needed per butene molecule formed, it is thus possible to rationalize the low amount of butene experimentally observed. It is important also to notice that

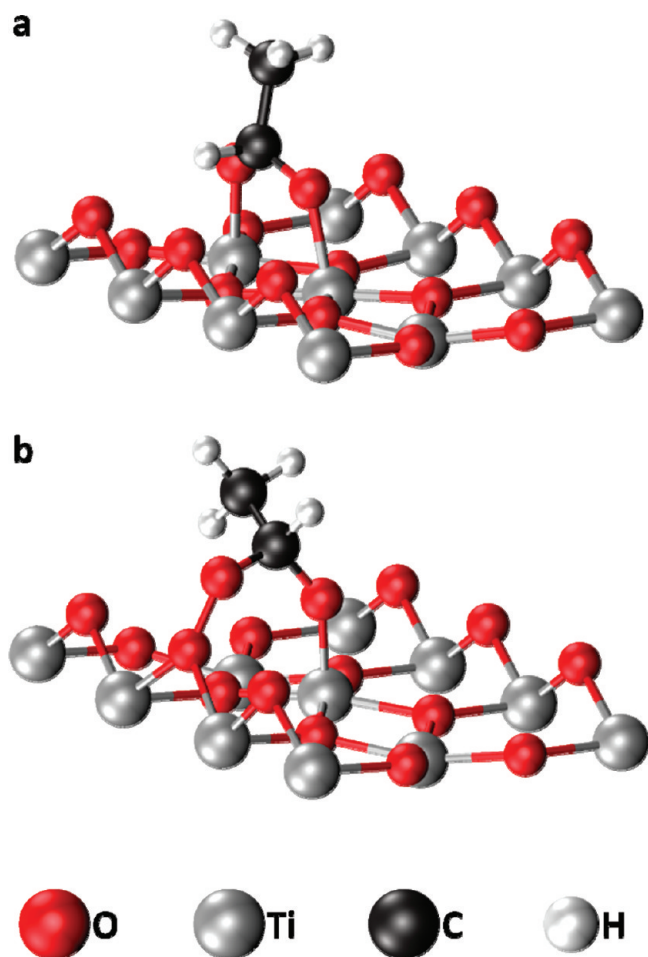


Figure 4. Adsorption geometries for the O-acetaldehyde complexes found on the TiO_2 surface. (a) After coordination to an O_{ad} adatom. (b) After coordination to an O_2 molecule adsorbed on a V_{O} site.

formation of butene is not a catalytic process. The V_{O} sites are active centers on this reaction that are consumed and not regenerated during the process.

Experimental TPD data for acetaldehyde adsorption on an oxygen precovered TiO_2 (110) reduced surface shows both a sensible stabilization of acetaldehyde at this surface and a detectable decomposition to form acetate. The low-coverage feature found at 320 K on the TPD on the reduced surface is shifted to 380 K on the oxidized surface, saturating at about 0.1 ML of coverage. On increasing coverage, a low-temperature peak develops at 345 K as a shoulder of the 380 K band and shifts downward to 240 K, saturating at a coverage of 1 ML. The same experimental data suggest that the barrier to acetate formation is low enough that O_2 dosed at room temperature has enough internal energy to initiate the reaction to form acetate. However, formation of acetate is a minor reaction channel as the majority of acetaldehyde desorbs molecularly on TPD. Our results indicate that upon reaction between an acetaldehyde molecule and an oxidized TiO_2 (110) surface at least the two O-acetaldehyde complexes depicted in Figure 4 may result. Complex **4a** is more stable by only 0.17 eV, so both kinds of complexes may coexist at the TiO_2 surface. Formation of either one is probably a complex process that depends, in part, not only on how the acetaldehyde molecule lands on the surface but also on details of the surface structure. Exploration of different paths for formation of either

complex shows that complex **4a** may result from reaction of an adsorbed acetaldehyde molecule and a O_{ad} adatom but requires surmounting a barrier of 1.25 eV. In this complex the acetaldehyde H_{α} atom is directly pointing toward an O_{b} atom, and complex deprotonation is found to be an easy, practically barrierless (0.03 eV) process. This results in formation of an adsorbed acetate on the $\text{Ti}_{5\text{c}}$ channel and an hydroxyl on the O row. A concerted process, i.e., complex formation with simultaneous deprotonation, is even easier, with a barrier of only 0.97 eV. This may explain the easiness of formation of acetate found experimentally. However, desorption of acetaldehyde from this final state is not easy. The acetate is highly stabilized on the TiO_2 (110) surface (-4.24 eV with respect to **4a** complex). Thus, this path may explain formation of acetate but not the additional stabilization of acetaldehyde found in TPD. The path for formation of complex **4b** found involves an acetaldehyde molecule adsorbed on the $\text{Ti}_{5\text{c}}$ channel and an O_2 molecule on a V_{O} site. Formation of this complex is barrierless (0.05 eV), and no deprotonation is possible as the distance between the acetaldehyde H_{α} atom and the nearby O_{b} atom is >4 Å. Molecular desorption of acetaldehyde is possible from this complex, with a barrier of 1.06 eV, which is quantitatively consistent with the stabilization seen in experimental TPD data.

CONCLUSIONS

In the present work a systematic study of the adsorption of acetaldehyde at the TiO_2 (110) rutile surface has been carried out by means of plane-wave pseudopotential DFT calculations. The adsorption geometries and energetics for a single acetaldehyde molecule on models of stoichiometric, reduced, and oxidized TiO_2 (110) surfaces have been examined. The computed desorption energy closely matches experimental TPD data on the reduced surface. The experimentally observed downward shift of the TPD signal on increasing surface coverage has been rationalized on the basis of the bonding mechanism that implies some degree of surface reduction by the adsorbed acetaldehyde molecules. This partial reduction of the surface results in a smaller interaction with newly incoming acetaldehyde molecules. Although limitations in pure GGA functional may result in an excessive charge delocalization on the $\text{Ti}_{5\text{c}}$ channels, it is found that a GGA+U treatment essentially does not modify the interpretation of this effect. The thermal reactivity of acetaldehyde on reduced and oxidized TiO_2 (110) surface models has been also examined. It has been found that acetaldehyde molecules adsorb preferentially on V_{O} sites on the reduced surfaces and that these acetaldehyde molecules may diffuse along the O_{b} row with a barrier that can be easily overcome at low temperatures. It is also found that when two acetaldehyde molecules that diffuse along the O_{b} row collide they may react and form in a barrier-free process an adsorbed butene complex. Further desorption of this butene complex requires rupture of two C–O bonds and simultaneous formation of the C–C π bond and thus implies a barrier that is estimated to be 1.38 eV. A first-order Redhead analysis shows that this desorption energy barrier will closely match the experimentally desorption temperature of 530 K. It is important also to notice that formation of butene is not a catalytic process. The V_{O} sites are active centers on this reaction that are consumed and not regenerated during the process. On an oxidized surface models of two O-acetaldehyde complexes have been found. The computed energies of these two complexes differ only in 0.17 eV, indicating that both

may coexist at the surface. The first complex is found to be formed through a path that involves reaction of an acetaldehyde molecule and an O_{ad} adatom on the Ti_{5c} channel. This complex easily loses its α -hydrogen and becomes an adsorbed acetate, highly stabilized on the surface. This explains the experimental observation of acetate desorption from oxidized TiO_2 surfaces at high temperatures. The second complex is formed through a path that involves an adsorbed acetaldehyde molecule and an O_2 molecule adsorbed on a V_O site. This second complex does not deprotonate, and the estimated barrier for desorption of acetaldehyde serves to explain the experimentally observed stabilization of the TPD traces of acetaldehyde on oxidized TiO_2 surfaces.

AUTHOR INFORMATION

Corresponding Author

*E-mail: marquez@us.es.

ACKNOWLEDGMENT

This work was funded by the Spanish Ministry of Science and Innovation, MICINN (grants MAT2008-04918, CSD2008-0023), and the Junta de Andalucía (P08-FQM-3661). Computational resources were provided by the Centro Nacional de Supercomputación-Barcelona Supercomputing Center (Spain). This work has benefited from the support of COST Action D37 ("GridChem").

REFERENCES

- (1) Henrich, V.; Cox, P. *The Surface Science of Metal Oxides*; Cambridge University Press: Cambridge, U.K., 1994.
- (2) Linsebigler, A. L.; Lu, G.; Yates, J. T. *Chem. Rev.* **1995**, *95*, 735.
- (3) Henry, C. R. *Surf. Sci. Rep.* **1998**, *31*, 231.
- (4) Diebold, U. *Surf. Sci. Rep.* **2003**, *48*, 53.
- (5) Thompson, T. L.; Yates, J. T. *Chem. Rev.* **2006**, *106*, 4428.
- (6) Pang, C. L.; Lindsay, R.; Thornton, G. *Chem. Soc. Rev.* **2008**, *37*, 2328.
- (7) Diebold, U.; Li, S.-C.; Schmid, M. *Annu. Rev. Phys. Chem.* **2010**, *61*, 129.
- (8) Du, Y.; Deskins, N. A.; Zhang, Z.; Dohnalek, Z.; Dupuis, M.; Lyubinetzky, I. *Phys. Chem. Chem. Phys.* **2010**, *12*, 6337.
- (9) Liu, L.-M.; Crawford, P.; Hu, P. *Prog. Surf. Sci.* **2009**, *84*, 155.
- (10) Henderson, M. A.; Epling, W. S.; Perkins, C. L.; Peden, C. H. F.; Diebold, U. *J. Phys. Chem. B* **1999**, *103*, 5328.
- (11) Epling, W. S.; Peden, C. H. F.; Henderson, M. A.; Diebold, U. *Surf. Sci.* **1998**, *412–413*, 333.
- (12) Wendt, S.; Sprunger, P. T.; Lira, E.; Madsen, G. K. H.; Li, Z.; Hansen, J. O.; Natthiesen, J.; Blekinge-Rasmussen, A.; Laegsgaard, E.; Hammer, B.; Besenbacher, F. *Science* **2008**, *320*, 1755.
- (13) Henderson, M. A.; White, J. M.; Uetsuka, H.; Onishi, H. *J. Am. Chem. Soc.* **2003**, *125*, 14974.
- (14) Matthey, D.; Wang, J. G.; Wendt, S.; Matthiesen, J.; Schaub, R.; Laegsgaard, E.; Hammer, B.; Besenbacher, F. *Science* **2007**, *315*, 1692.
- (15) Kiennemann, A.; Idriss, H.; Kieffer, R.; Chaumette, P.; Durand, D. *Ind. Eng. Chem. Res.* **1991**, *30*, 1130.
- (16) Idriss, H.; Diagne, C.; Hindermann, J. P.; Kiennemann, A.; Barteau, M. A. *J. Catal.* **1995**, *155*, 219.
- (17) Martins, E. M.; Correa, S. M.; Arbilla, G. *Atmos. Environ.* **2003**, *37*, 23.
- (18) Colón, M.; Pleil, J. D.; Hartlage, T. A.; Guardini, M. L.; Martins, M. H. *Atmos. Environ.* **2001**, *35*, 4017.
- (19) Meroni, D.; Ardizzone, S.; Cappelletti, G.; Oliva, C.; Ceotto, M.; Poelman, D.; Poelman, H. *Catal. Today*, **2010**, in press; doi:10.1016/j.cattod.2010.08.13
- (20) Fujishima, A.; Zhang, X.; Tryk, D. A. *Surf. Sci. Rep.* **2008**, *63*, 515.
- (21) Zehr, R. T.; Henderson, M. A. *Surf. Sci.* **2008**, *602*, 2238.
- (22) Thompson, T. L.; Yates, J. T., Jr. *Chem. Rev.* **2006**, *106*, 4428.
- (23) Kresse, G.; Hafner, J. *Phys. Rev. B* **1996**, *47*, 558–561.
- (24) Kresse, G.; Furthmüller, J. *Comput. Mater. Sci.* **1996**, *6*, 15.
- (25) Kresse, G.; Furthmüller, J. *Phys. Rev. B* **1996**, *54*, 11169–11186.
- (26) Blöchl, P. E. *Phys. Rev. B* **1994**, *50*, 17953–17979.
- (27) Kresse, G.; Joubert, D. *Phys. Rev. B* **1999**, *59*, 1756–1775.
- (28) Perdew, J. P.; Chevary, J. A.; Vosko, S. H.; Jackson, K. A.; Pederson, M. R.; Singh, D. J.; Fiolhais, C. *Phys. Rev. B* **1992**, *46*, 6671–6687.
- (29) Harris, J. *Phys. Rev. B* **1985**, *31*, 1770–1779.
- (30) Henkelman, G.; Uberuaga, B. P.; Jonsson, H. *Comput. Mater. Sci.* **2006**, *36*, 354–360.
- (31) Márquez, A. M.; Plata, J. J.; Fdez. Sanz, J. J. *Phys. Chem. C* **2009**, *113*, 19973.
- (32) Rasmussen, M. D.; Molina, M. L.; Hammer, B. J. *Chem. Phys.* **2004**, *120*, 14583.
- (33) Tilocca, A.; Selloni, A. *ChemPhysChem* **2005**, *6*, 1991.
- (34) Deskins, N. A.; Rousseau, R.; Dupuis, M. *J. Phys. Chem. C* **2010**, *114*, 5891.
- (35) Di Valentin, C.; Pacchioni, G.; Selloni, A. *Phys. Rev. Lett.* **2006**, *97*, 166803.
- (36) Pacchioni, G. *J. Chem. Phys.* **2008**, *128*, 182505.
- (37) Deskins, N. A.; Dupuis, M. *Phys. Rev. B* **2007**, *75*, 195212.
- (38) Calzado, C. J.; Hernández, N. C.; Sanz, J. F. *Phys. Rev. B* **2008**, *77*, 045118.
- (39) Ganduglia-Pirovano, M. V.; Hofmann, A.; Sauer, J. *Surf. Sci. Rep.* **2007**, *62*, 219.
- (40) Dudarev, S. L.; Botton, G. A.; Savrasov, S. Y.; Humphreys, C. J.; Sutton, A. P. *Phys. Rev. B: Condens. Matter Phys.* **1998**, *57*, 1505.
- (41) Deskins, N. A.; Rousseau, R.; Dupuis, M. *J. Phys. Chem. C* **2009**, *113*, 14583.
- (42) Park, J. B.; Graciani, J.; Evans, J.; Stacchiola, D.; Ma, S. G.; Liu, P.; Nambu, A.; Sanz, J. F.; Hrbeek, J.; Rodriguez, J. A. *Proc. Natl. Acad. Sci.* **2009**, *106*, 4975–4980.
- (43) Redhead, P. A. *Vacuum* **1962**, *12*, 203.